The Plant Journal (2005) **41**, 567–582 doi: 10.1111/j.1365-313X.2004.02321.x

Functional distribution and dynamics of Arabidopsis SR splicing factors in living plant cells

Vinciane Tillemans[1,†], Laurence Dispa[1], Claire Remacle[2], Mélanie Collinge[1] and Patrick Motte[1,3,*,†]
[1]*Laboratory of Plant Cell and Molecular Biology,*
[2]*Genetics of Microorganisms, Department of Life Sciences, and*
[3]*Center for Assistance in Technology of Microscopy (CATM), University of Liège, B-4000 Liège, Belgium*

Received 1 October 2004; revised 15 November 2004; accepted 19 November 2004.
[*]For correspondence (fax +3243662960; e-mail patrick.motte@ulg.ac.be).
[†]These authors contributed equally to this work.

Summary

Serine/arginine-rich (SR) proteins constitute an important class of splicing regulators in higher eukaryotes that share a modular structure consisting of one or two N-terminal RNA recognition motif (RRM) domains and a C-terminal RS-rich domain. Herein, we have investigated the *in vivo* functional distribution of Arabidopsis SR factors. *Agrobacterium*-mediated transient transformation revealed nuclear speckled distribution and the overall colocalization of fluorescent protein (FP)-tagged SR factors in both tobacco and Arabidopsis cells. Their overall colocalization in larger nucleoplasmic domains was further observed after transcriptional and phosphorylation/dephosphorylation inhibition, indicating a close functional association between SR factors, independent of their phosphorylation state. Furthermore, we demonstrated *in vivo* the conserved role of the RS and RRM domains in the efficient targeting of Arabidopsis SR proteins to nuclear speckles by using a series of structural domain-deleted mutants of atRSp31 and atRSZp22. We suggest additional roles of RS domain such as the shuttling of atRSZp22 between nucleoplasm and nucleolus through its phosphorylation level. The coexpression of deletion mutants with wild-type SR proteins revealed potential complex associations between them. Fluorescence recovery after photobleaching demonstrated similar dynamic properties of SR factors in both tobacco transiently expressing cells and Arabidopsis transgenics. Cell cycle phase-dependent organization of FP-tagged SR proteins was observed in living tobacco BY-2 cells. We showed that atRSp31 is degraded at metaphase by fluorescence quantification. SR proteins also localized within small foci at anaphase. These results demonstrate interesting related features as well as potentially important differences between plant and animal SR proteins.

Keywords: pre-mRNA splicing, nuclear speckles, SR proteins, Arabidopsis, cell cycle, transient expression.

Introduction

Pre-mRNA splicing is catalysed by the spliceosome consisting of small nuclear ribonucleoprotein particles (snRNPs) as well as numerous additional proteins (Brown and Simpson, 1998; Kramer, 1996; Reddy, 2001). Among the non-snRNP splicing factors, the family of serine- and arginine-rich (SR) proteins is required for the accurate spliceosome assembly (Graveley, 2000). SR proteins are characterized by similar structural features including one or two RNA recognition motifs (RRM) at their N termini and an Arg/Ser repeat domain (RS) at their C termini. In humans, there are at least 10 SR proteins including the well-characterized ASF/SF2, SC35 and 9G8 factors (Graveley, 2000). The survey of the Arabidopsis genome led to the identification of at least 19 genes encoding distinct SR factors belonging to several (sub)classes (Kalyna and Barta, 2004).

Serine/arginine-rich proteins are non-randomly organized within metazoan nuclei and localize to irregularly shaped speckles (or splicing factor compartments). Time-lapse microscopy has shown that their nuclear distribution is complex and highly dynamic, and may constitute an additional level of gene expression regulation (reviewed in Lamond and Spector, 2003). Metazoan speckles correspond to a pool of splicing factors which can be recruited to the sites of high transcriptional activity (Melcak *et al.*, 2000). In

electron microscopy, the mammalian speckles correspond to interchromatin granule clusters and perichromatin fibrils (Sacco-Bubulya and Spector, 2002). The relocation of mammalian SR factors from speckles to actively transcribed genes depends on their phosphorylation state (Misteli, 2000).

In contrast to the extensive knowledge on the compartmentalization of pre-mRNA processing factors in metazoa, very little is known about the topic in plants. We previously observed a speckled organization of atRSp31 in germinating seeds by using immunofluorescence microscopy and green fluorescent protein (GFP) translational fusion (Docquier *et al.*, 2004). Small or micro-clusters of interchromatin granules have been observed as well in differentiated Arabidopsis cells and correspond to SR protein-containing speckles (Docquier *et al.*, 2004; Fang *et al.*, 2004). However, the functional organization and dynamics of many SR splicing factors in plant nuclei remain unknown. For example, whether (and to what extent) SR proteins colocalize within the same nuclear territories in interphase cells, which protein domain is important for spatial targeting or whether the localization of SR proteins is regulated in a cell cycle phase-dependent manner are still unknown features of plant SR proteins. Herein, we develop a fluorescent protein (FP)-based assay to investigate the functional dynamics of Arabidopsis SR factors by using confocal imaging and transient expression. Our findings suggest the overall nucleoplasmic colocalization of SR factors despite slight differences in their nuclear distribution. However, unexpectedly, we also found atRSZp22 in the nucleolus and the significance of this localization is discussed within the context of mRNA export. The role of different domains of SR proteins in their subcellular distribution was also investigated. While confirming the role of the RS domain in speckle targeting, our study reveals interesting properties of Arabidopsis SR protein domains. We also demonstrate that transient expression of FP-tagged proteins coupled with the use of fluorescence recovery after photobleaching (FRAP) is a versatile approach for investigating the dynamics of splicing factors in living plant cells.

Very little is known about the cellular reorganization of splicing factors, including SR proteins, during the plant cell cycle (Boudonck *et al.*, 1998, 1999). We therefore expressed FP-tagged SR proteins in transgenic tobacco BY-2 cells to investigate their subcellular localization and dynamics during the cell cycle.

Results

Transient (co)expression of SR splicing factors organize into nuclear speckles

We previously suggested that agroinfiltration-mediated transient expression can provide a suitable approach to investigate the subcellular distribution of plant SR factors without needing to generate protoplasts prior to transformation (Docquier *et al.*, 2004). In order to analyse the compartmentalization of various Arabidopsis splicing regulators (atRSp31, atSRp34, atRSZp22 and atRSZ33), leaf cells were inoculated with *Agrobacterium* strains containing the appropriate construct (Figure 1a). SR proteins showed a nuclear localization with a 'speckled' pattern after transient transformation of both tobacco and Arabidopsis cells (Figure 1b). The diffuse fraction often appeared slightly more intense in tobacco nuclei (Figure 1b). Interestingly, the use of a heterologous transient expression assay demonstrates that the presence of endogenous Arabidopsis SR proteins is dispensable for the speckled organization of SR factors. Slight differences in the shape of the speckles could sometimes be observed between diverse SR proteins. This observation was more apparent with atRSZ33 which seemed to be present in long intranuclear tracks connecting irregularly shaped speckles contrary to atRSp31 which formed more dot-like speckles. We do not know the functional significance, if any, of such slight differences. Similar to our previous observations on transgenic seedlings (Docquier *et al.*, 2004), we observed movements of the fusion proteins at the periphery of the speckles which could also display some budding over time in transiently expressing cells. In some nuclei, atRSZp22 was faintly detected in the nucleolus (Figure 2). As mentioned in Experimental procedures,

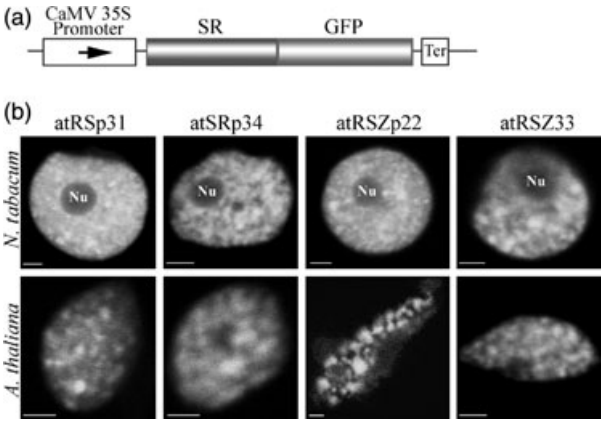

Figure 1. Arabidopsis SR protein localization in leaf nuclei after *Agrobacterium*-mediated transient transformation.
(a) Diagram of the binary constructs used for *Agrobacterium*-mediated transient transformation in tobacco and Arabidopsis leaf cells. The chimeric constructs consist of the SR protein coding sequences fused with GFP at the 3′ side in an in-frame manner. Expression is driven by the CaMV35S promoter. All constructs are either in the binary vector pBAR35S or in the vector pBIN121, which contain, respectively, the CaMV35S promoter and terminator (Ter) and the glufosinate ammonium resistance gene, and the CaMV35S promoter, a kanamycin resistance gene and the polyadenylation signal from the nopaline synthase gene (Ter).
(b) Confocal images of GFP-tagged SR proteins transiently expressed in *Nicotiana tabacum* and *Arabidopsis thaliana*. Splicing SR factors localize specifically in a speckled pattern and diffusely in the nucleoplasm but are excluded from nucleoli (Nu). Scale bar, 2 μm.

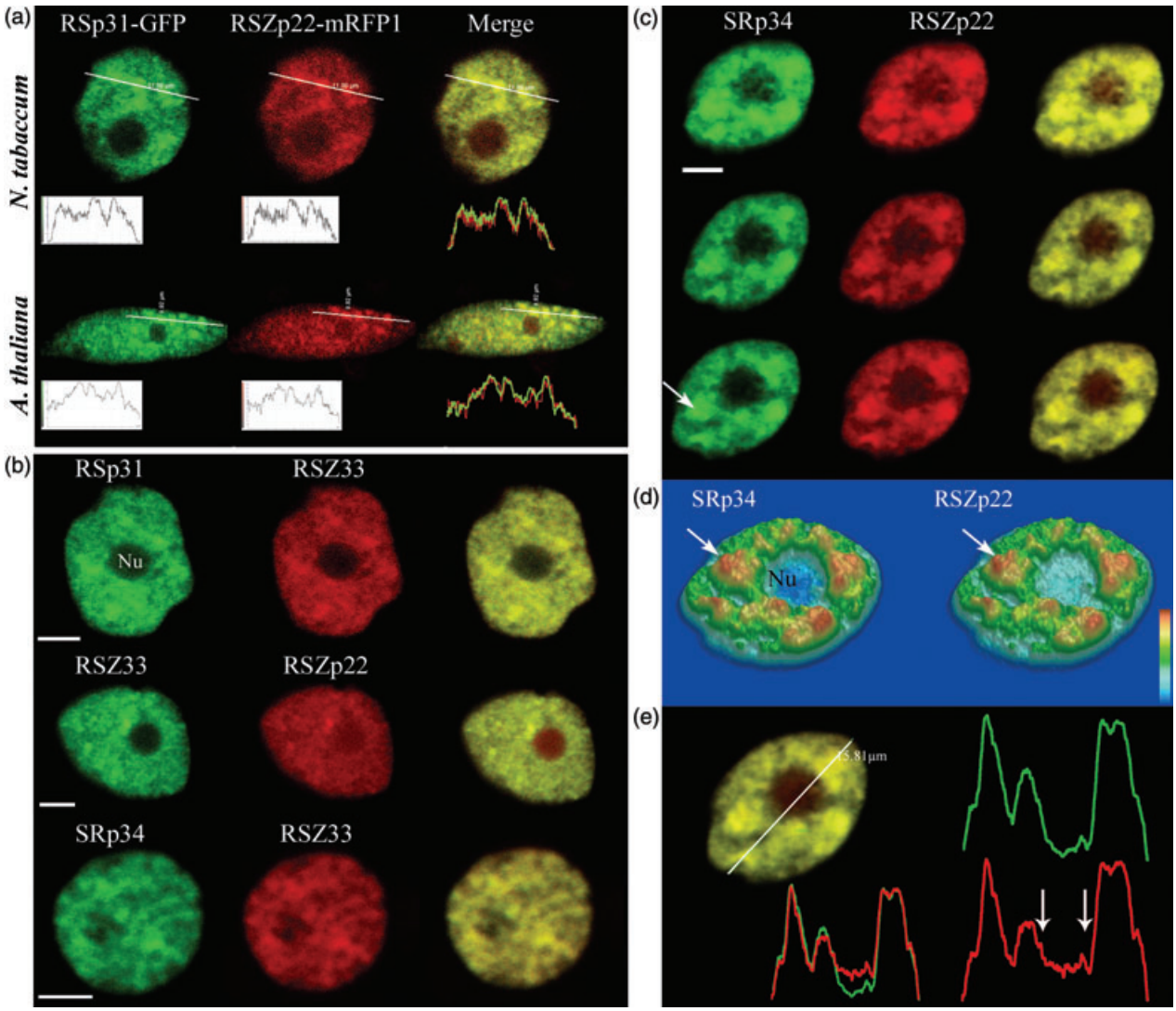

Figure 2. Colocalization of SR factors after *Agrobacterium*-mediated transient coexpression. The left and middle panels correspond to individual colour channels and the right panel is the overlay.
(a) Coexpression of atRSp31-GFP (green) and atRSZp22-mRFP1 (red) in both tobacco and Arabidopsis leaf cells shows that the green fluorescent signals clearly overlap with the red one in both species, as demonstrated by the relative intensity fluorescence profiles plotted along the line.
(b) Nuclear colocalization of transiently expressed atRSp31-GFP with atRSZ33-mRFP1 and atRSZ33-GFP with atRSZp22-mRFP1 and at SRp34-GFP with atRSZ33-mRFP1 in tobacco leaf cells. Note the fluorescence of atRSZp22 in the nucleolus.
(c–e) Selection of confocal images through the same nucleus expressing atSRp34-GFP and atRSZp22-mRFP1. The arrow points to the same speckle. As shown in the colour coded 3-D topological images of fluorescence intensities (d), both SR factors are enriched in the same nuclear domains with the same relative concentration.
(e) The relative fluorescence intensities along the line segment show nearly identical concentration of fluorescent protein-tagged SR proteins except for atRSZp22 which is also visible in the nucleolus (position marked by arrows). Scale bar, 4 µm.

a rather long period of observation led to an unusual distribution of FP-tagged SR proteins resembling the one induced after inhibitor treatments (see later results). Under these experimental stresses, atRSZp22 strongly accumulated in the nucleoli while atRSp31 localized more around it (Figure S1).

Although a speckled distribution of plant SR proteins is now emerging, nothing is known about their possible association within the nucleus. The general nuclear speckled distribution prompted us to investigate whether they are all targeted to the same domains. Therefore, we studied the colocalization of different couples of SR proteins by using GFP and mRFP1 translational fusions. First, atRSp31-GFP and atRSZp22-mRFP1 were simultaneously coexpressed in tobacco and Arabidopsis cells (Figure 2a). The merging of GFP and mRFP1 signals showed a similar distribution pattern and a colocalization in the same nuclear territories in both tobacco and Arabidopsis cells as demonstrated by the quantification of fluorescence by using profiles of fluorescence intensities along line segments (Figure 2a).

Tobacco was preferentially used for coexpression experiments due to the highest cell transformation efficiency. Next, we examined the distribution of other coexpressed SR proteins and, as obvious from Figure 2, they colocalized in the nucleoplasm with the exception of atRSZp22-mRFP1 which could sometimes be detected in the nucleoli. When coexpressed in the same nuclei, SR proteins accumulated in slightly larger speckles which can show an intermediate shape/morphology between the one observed for each individual SR protein (Figure S2).

Previous studies showed that blocking of transcription and phosphorylation/dephosphorylation cycle causes redistribution of distinct SR proteins in the nucleus (Ali *et al.*, 2003; Docquier *et al.*, 2004; Savaldi-Goldstein *et al.*, 2000). To determine whether the colocalization of SR proteins is dependent on transcriptional activity, cells coexpressing SR proteins (atRSp31-GFP and atRSZp22-mRFP1, atSRp34 and atRSZp22, atSRp34 and atRSZ33) were treated with the transcriptional inhibitor α-amanitin. A similar redistribution of FP-tagged SR splicing factors in large areas, often surrounding the nucleolus, was found following this treatment (Figure 3). AtRSp31and atRSZp22 redistributed in very bright and large round speckles concomitantly with the disappearance of the diffuse fraction after a longer period of treatment (Figure 3).

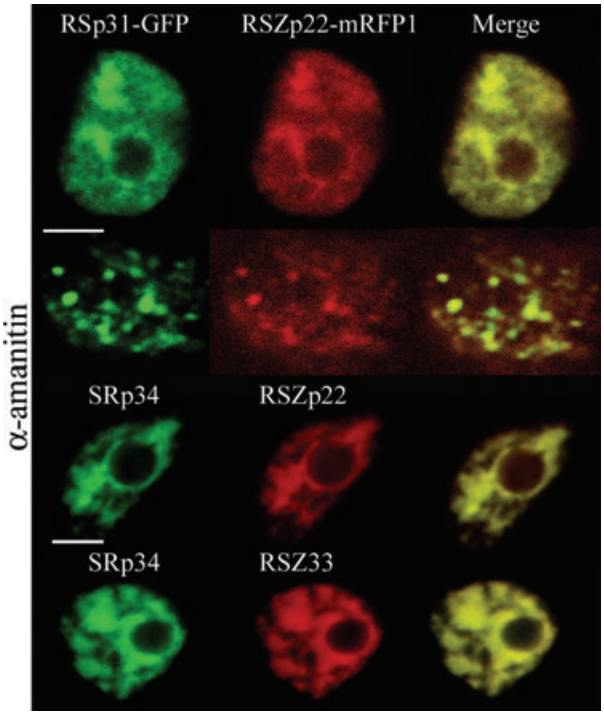

Figure 3. Treatments with the transcriptional inhibitor α-amanitin affect subnuclear distribution of SR factors but not their colocalization. Confocal images show the coexpression in tobacco nuclei of atRSp31-GFP with atRSZp22-mRFP1 (upper panels, after 3 or 7 h of treatment), atSRp34-GFP with atRSZp22-mRFP1 (middle panel) and of atSRp34-GFP with atRSZ33 (lower panel). Scale bar, 4 μm.

As SR protein interactions can be differentially affected by reversible phosphorylation *in vitro* and *in vivo* (Savaldi-Goldstein *et al.*, 2000; Yeakley *et al.*, 1999), we next questioned whether okadaic acid and staurosporine (respectively Ser/Thr protein phosphatase and kinase inhibitors) treatments induce a change in the distribution pattern of SR factors. Exposure of transiently coexpressing cells to these inhibitors caused atRSp31 and atRSZp22 to relocalize to the same nuclear domains (Figure 4). Fluorescence of the diffusion fraction decreased and the speckles were larger, coalesced and organized around the nucleolus (Figure 4). Upon a longer staurosporine treatment, atRSZp22 finally accumulated in the nucleolus although the two SR proteins were still targeted to the same domains within the nucleoplasmic fraction (Figure 4). By comparison, when expressed alone, atRSZp22 concentrated in the nucleolus while atRSp31 accumulated in perinucleolar domains (Figure 5e and Figure S3).

When coexpressed, a similar reorganization was observed for atRSp34 and atRSZp22 after inhibitor treatment

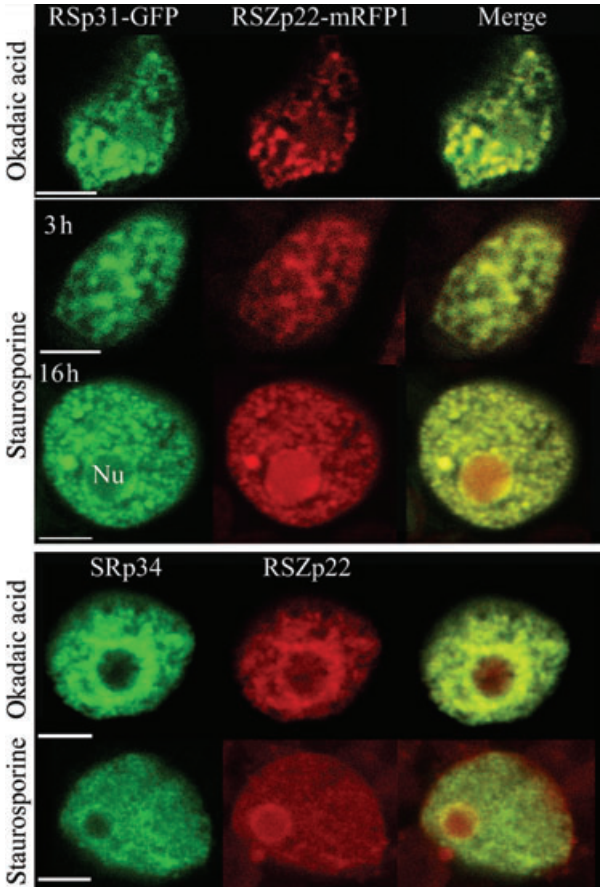

Figure 4. Redistribution of co-expressed FP-tagged Arabidopsis SR proteins (atRSp31-GFP with atRSZp22-mRFP1, atSRp34-GFP with atRSZp22-mRFP1, after treatment with okadaic acid, an inhibitor of Ser/Thre phosphatases and with staurosporine, an inhibitor of protein kinases after 3 or 16 h of treatment for RSp31 and RSZp22). Scale bar, 4 μm.

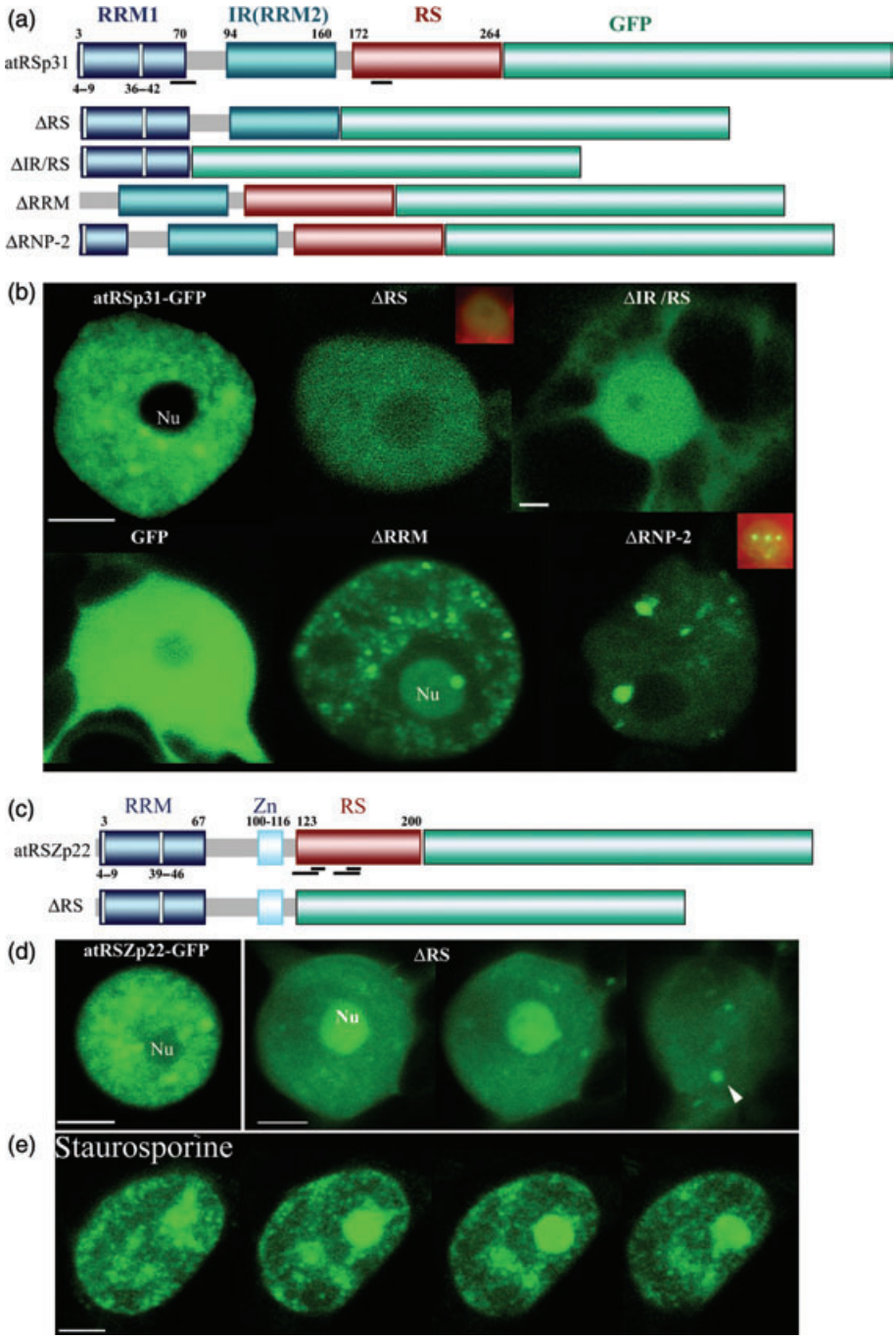

Figure 5. Role of Arabidopsis SR protein structural domains in cellular and subnuclear localization.
(a) Schematic drawing of the structural domains of atRSp31; representations of mutants with deletion of the RS domain, the IR/RS domains, the RRM domain and the RNP2 motif of RRM1 are shown in order below that of atRSp31-GFP (drawn to scale). The analysis of the primary sequence using PSORT program (http://psort.nibb.ac.jp/form.html) indicated a putative bipartite nuclear localization signal (NLS) beginning at Lys-64 and a monopartite NLS beginning at Pro-184 (or Arg-187). The putative NLSs are underlined, and the amino acid numbers indicate the position of the domains and of the RNP motifs (vertical thin white lines).
(b) Confocal microscopy of tobacco nuclei expressing atRSp31-GFP and the mutant proteins (see text for detailed description). The insets are epifluorescence images.
(c) Scheme of the structural domains of atRSZp22, fused to GFP and the ΔRS mutant protein (drawn to scale). The analysis of atRSZp22 primary sequence indicated many putative bipartite and monopartite NLSs, all located in the RS domain (beginning from Arg-121 and ending at Pro-155).
(d) Fluorescence distribution of wild-type atRSZp22 (left) and selection of optical serial sections through a nucleus expressing atRSZp22ΔRS (right) demonstrating the overall diffuse localization of the mutant protein in cytoplasm and nucleoplasm and its concentration into nucleoli. Some bright foci are visible (arrowhead).
(e) Selection of optical serial sections showing the nucleolar accumulation of atRSZp22 in the entire nuclear depth after staurosporine treatment, suggesting the role of the RS domain in nucleolar localization through its phosphorylation level. Nu, nucleolus. Scale bar, 4 μm.

(Figure 4). Staurosporine treatment for a longer period induced atRSZp22 to accumulate in the nucleolus as well. The finding that SR proteins are re-targeted to new nuclear domains in response to nuclear architecture changes (probably through a new network of interactions with other nuclear components) and remain associated after inhibitor treatments could reflect functional associations between SR proteins in either tobacco or Arabidopsis cells.

Expression of SR deletion mutants leads to aberrant subcellular distribution

RS domains have been reported to be sufficient for speckle localization for a subset of SR and SR-related proteins (Cazalla *et al.*, 2002; Gama-Carvalho *et al.*, 1997). Nothing, however, is known about the importance of Arabidopsis SR protein domains for spatial targeting within the plant nucleus. We investigated which structural domains of SR proteins are required for their nuclear targeting and speckled distribution. AtRSp31 is characterized by the presence of one N-terminal RRM, an intermediate RRM and a C-terminal RS domain (Figure 5a) (Lopato *et al.*, 1996). The analysis of the primary sequence (PSORT program) indicated putative bipartite and monopartite nuclear localization signals located in the RS domain. Mutant proteins, in which either the RS domain alone (atRSp31ΔRS) or the intermediate and RS domains were deleted (atRSp31ΔRI/RS, see Figure 5a), were distributed in the nucleus (excluding nucleolus) and cytoplasm (Figure 5b). FP-tagged mutant proteins lacking the RS domain failed to organize in a speckled pattern, and displayed faint fluorescence in both tobacco and Arabidopsis cells (as shown in the epifluorescence image inset of Figure 5b, upper row). The decrease of fluorescence suggests a role of the RS domain in the stability of the atRSp31 protein possibly due to a folding problem of the fusion protein. The deletion mutant lacking the N-terminal RRM (atRSp31ΔRRM) localized to the nucleus and concentrated into larger speckles (Figure 5b). Time-lapse confocal microscopy showed an alternating fluorescence of the nucleoli, indicating that atRSp31ΔRRM proteins were shuttled between the nucleoplasm and nucleoli. We investigated next whether the deletion of the half N-terminal RRM domain containing the RNP-2 submotif affects the subcellular localization of atRSp31. The distribution of atRSp31ΔRNP-2 appeared mainly as large aggregates (often two or three, see the epifluorescence image inset of Figure 5b, lower row) with bright fluorescence, sometimes associated with the nucleolus. This finding showed that the removal of only the first half N-terminal RRM containing the RNP-2 submotif has a dramatic effect on the subcellular localization of the mutant protein consistent with previous studies showing that amino acid substitutions within the RNP motifs greatly diminish RNA-protein interactions (Gama-Carvalho *et al.*, 2001).

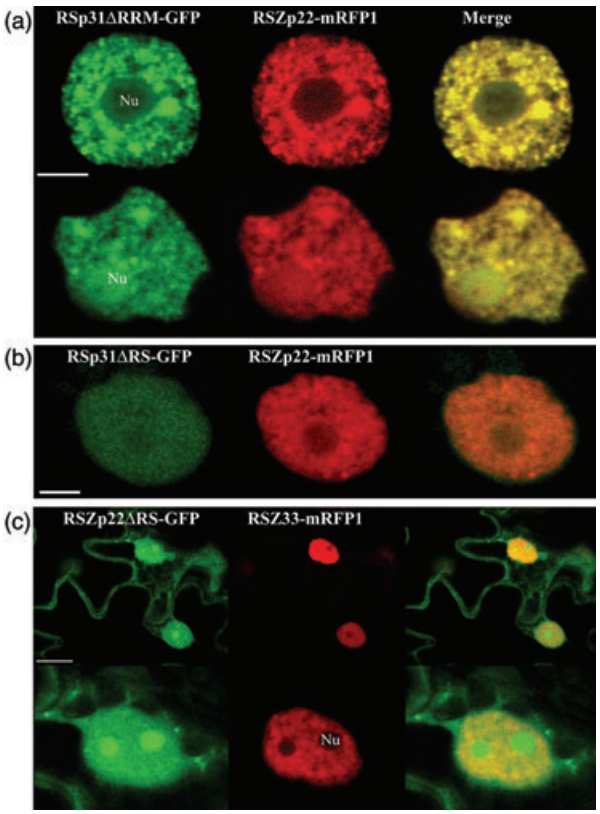

Figure 6. Co-localization of transiently expressed mutant with wild-type SR proteins in tobacco nuclei. The panels at right show colour overlays of atRSp31ΔRRM-GFP with atRSZp22-mRFP1 (a), atRSp31ΔRS-GFP with atRSZp22-mRFP1 (b) and atRSZp22ΔRS-GFP with atRSZ33-mRFP1 (c). Nu, nucleolus. Scale bar: (a, b) 4 μm, (c) 16 μm.

The roles of the RS domain of atRSp31 in nuclear targeting, speckle distribution and protein stability prompted us to investigate the role of the RS domain from atRSZp22, an Arabidopsis Zn knuckle-containing SR factor (Figure 5a,c). The ectopically expressed atRSZp22ΔRS mutant protein localized both in the cytoplasm and in the nucleus (Figures 5 and 6). The deletion mutant failed to concentrate in the typical speckled pattern although rare foci could be observed in both the cytoplasm and the nucleus (Figures 5 and 6). Unexpectedly, atRSZp22ΔRS accumulated in the nucleoli independently of the period of observation and therefore not under experimental stress (Figure 5d, right image). In contrast to atRSp31, atRSZp22 strongly fluoresced in the absence of the RS domain (Figures 5 and 6).

Structural determinants for colocalization of Arabidopsis SR factors

To investigate the role of the individual domains of SR proteins in their colocalization *in vivo*, we coexpressed deletion forms of atRSp31 with wild-type atRSZp22 (Figure 6). AtRSp31ΔRS and atRSZp22 did not colocalize. Indeed,

atRSp31ΔRS diffusely distributed in the nuclei while atRSZp22 accumulated in speckles (Figure 6b). Similarly, the coexpression of atRSZp22ΔRS with atRSZ33 displayed a diffuse distribution pattern of atRSZp22ΔRS which concentrated in the nucleolus while atRSZ33 displayed the typical speckled pattern (Figure 6c). Thus, the deletion of the RS domain alters the colocalization of the SR proteins in transiently expressing cells (Figure 6). Surprisingly, coexpression of atRSZp22 with atRSp31ΔRRM mutant changed atRSZp22 intranuclear distribution, causing their colocalization in aberrant and numerous large or tiny foci and in the nucleolus (Figure 6a). AtRSp31ΔRRM seemed to drag along atRSZp22 into this particular distribution, suggesting the 'dominant' effect of the mutation in the colocalization of splicing factors.

Relationship between speckles and RNA polymerase II

Whether plant SR protein organization fits into the well-established model of nuclear compartmentalization and dynamics of mammalian cells is still unclear. In our previous report, we suggested that the speckled distribution of SR proteins might reflect a high and transient demand of splicing factors in response to actively transcribed genes rather than a reservoir of pre-mRNA factors (Docquier *et al.*, 2004). As pre-mRNA splicing has been shown to occur co-transcriptionally (Prasanth *et al.*, 2003), the colocalization of coexpressed SR factors and RNAP II within speckles would suggest that large speckles correspond to actively transcriptional sites. We used the agroinfiltration-based assay to assess this possibility. Rpb15.9 (one small subunit of Arabidopsis RNAP II; Larkin and Guilfoyle, 1998) was fused to GFP and expressed in tobacco and Arabidopsis leaf cells (Figure 7). Expressing cells first showed an intense cytoplasmic fluorescence and a weak nuclear one. Later (likely after passive diffusion of the fusion protein of approximately 47 KDa through the nuclear pore complexes) fluorescence was detected throughout the nucleoplasm with additional tiny foci (Figure 7). Although the functional

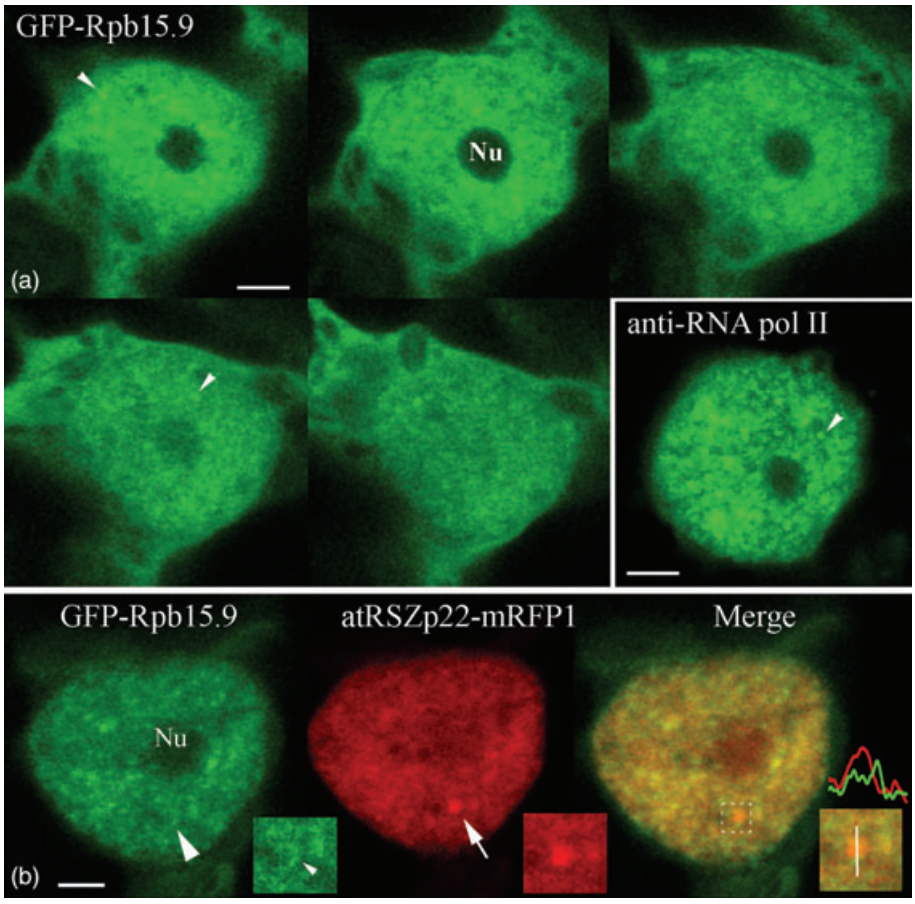

Figure 7. Nuclear distribution of GFP-Rpb15.9.
(a) Selection of serial optical sections through a tobacco nucleus transiently expressing GFP-Rpb15.9. Like the endogenous RNAP II detected by immunofluorescence (anti-RNA pol II, lower row, right image), GFP-Rpb15.9 shows a nuclear distribution with numerous tiny foci (arrowheads).
(b) Confocal section of one representative nucleus showing the colocalization of GFP-Rpb15.9 and atRSZp22-mRFP1. The image at right shows the colour overlay. Enlarged area (insets) shows that GFP-Rpb15.9 (arrowheads) can concentrate around nuclear speckles (arrow). The relative fluorescence intensities measured along the line are represented (see text for details). Nu, nucleolus. Scale bar, 4 μm.

association of GFP- Rpb15.9 in the RNAP II complex could not be assessed, Kimura *et al.* (2001) previously showed that GFP-tagged Rpb4 (the homologous subunit of Rpb15.9) complement a Rpb4 loss-of-function mutation in *Schizosaccharomyces pombe* (Kimura *et al.*, 2001). The distribution of GFP-Rpb15.9 was next compared with that of endogenous RNAP II by imunofluorescent labelling in Arabidopsis and tobacco cells using H5 anti-RNAP II antibodies which label only the active and hyperphosphorylated CTD of the catalytic subunit of RNAP II. RNAP II was detected exclusively in the nucleus where it was dispersed throughout the nucleoplasm and enriched in very small foci (Figure 7, lower row, right image), similar to GFP-tagged Rpb15.9. Thus, we simultaneously coexpressed GFP-Rpb15.9 and atRSZp22-mRFP1 (Figure 7b). Fusion proteins appeared to have a partial overlap of their distribution pattern in some nucleoplasmic areas and in tiny foci. There was no clear colocalization of Rpb15.9 and atRSZp22 in the speckles (Figure 7b). Confocal images showed that in some cells GFP-Rpb15.9 sometimes surrounds the periphery of the speckles (see insets and intensity profiles in Figure 7b). Highest resolution of electron microscopy would be required to further investigate the relationship between RNAP II and SR proteins.

SR proteins are highly dynamic splicing factors in interphase nuclei

The FRAP analysis has been widely used for tracking the movement of mammalian intranuclear proteins (Lamond and Spector, 2003; Phair and Misteli, 2000). We performed FRAP experiments on atRSp31-GFP stably expressing Arabidopsis seedlings previously generated in the laboratory (Figure 8a) (Docquier *et al.*, 2004). Regions of interest in atrichoblast and trichoblast nuclei were bleached and the kinetics of recovery, reflecting the mobility of atRSp31-GFP, was measured by sequential imaging (see Experimental procedures). As shown in Figure 8(b), recovery after photobleaching of a nucleoplasmic region was complete within 30 sec, with a half-time of approximately 5.7 sec. The recovery percentage, reflecting the mobility fraction, was relatively constant and ranged between 49 and 56% suggesting the apparent importance of immobile fraction. However, generation of stable transgenic plants is time consuming. Rates of fluorescence recovery of atRSp31-GFP were therefore compared between stable transgenics and heterologous tobacco transiently expressing cells to demonstrate the potential use of transient transformation in FRAP experiments. FRAP analysis was performed on tobacco leaf cells after agroinfiltration and very similar recovery rates (half-time of approximately 5.6 sec) were observed (Figure 8c) despite various physiological and putative differences in nuclear architecture between transiently expressing tobacco leaf cells and stably expressing Arabidopsis root cells. These findings show the prospective interest of using transiently expressing heterologous tobacco cells to study the dynamics of nuclear factors by using FRAP. We should note that the mobility fraction was slightly higher in transiently expressing cells than in stable transgenics (around 65%) which could be the consequence of a more important diffuse fraction in tobacco nuclei. The analysis of the mobility of atRSZ33 using FRAP showed again a rapid fluorescence recovery with a half-time of 5.1 sec in transiently expressing cells. As a control, FRAP was also performed on cells transiently expressing free GFP and the half-time of recovery was always under 1 sec. While this manuscript was in preparation, Fang *et al.* (2004) reported FRAP analysis of atSRp34 and SR33 in stable transgenics. Although these authors reported slightly faster recovery rates (half time recovery of 2.5 sec), our report substantiates the view that plant SR proteins are highly mobile within the nucleus.

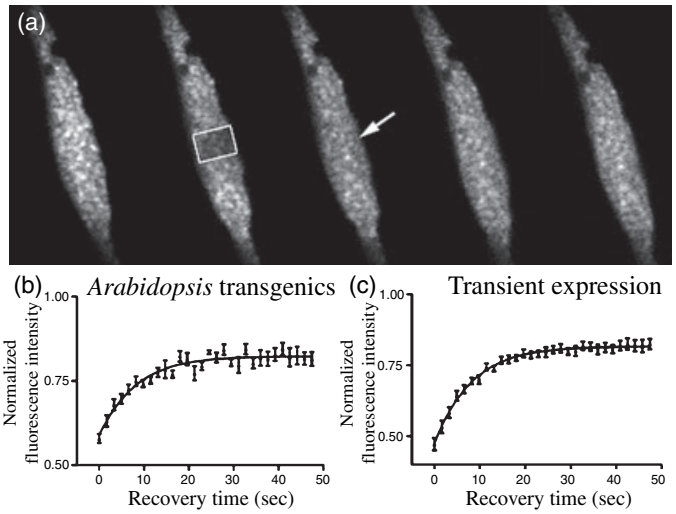

Figure 8. FRAP of atRSp31-GFP in stably and transiently transformed living cells.
(a) Epidermal cells were imaged before (pre-bleaching) and during recovery of fluorescence after photobleaching. The white rectangle shows the bleached area and the arrow the reappearance of the fluorescence.
(b) Kinetics of fluorescence recovery in Arabidopsis transgenics.
(c) Kinetics of fluorescence recovery in transiently expressing tobacco leaf cells. One hundred per cent fluorescence indicates pre-bleach fluorescence intensity.

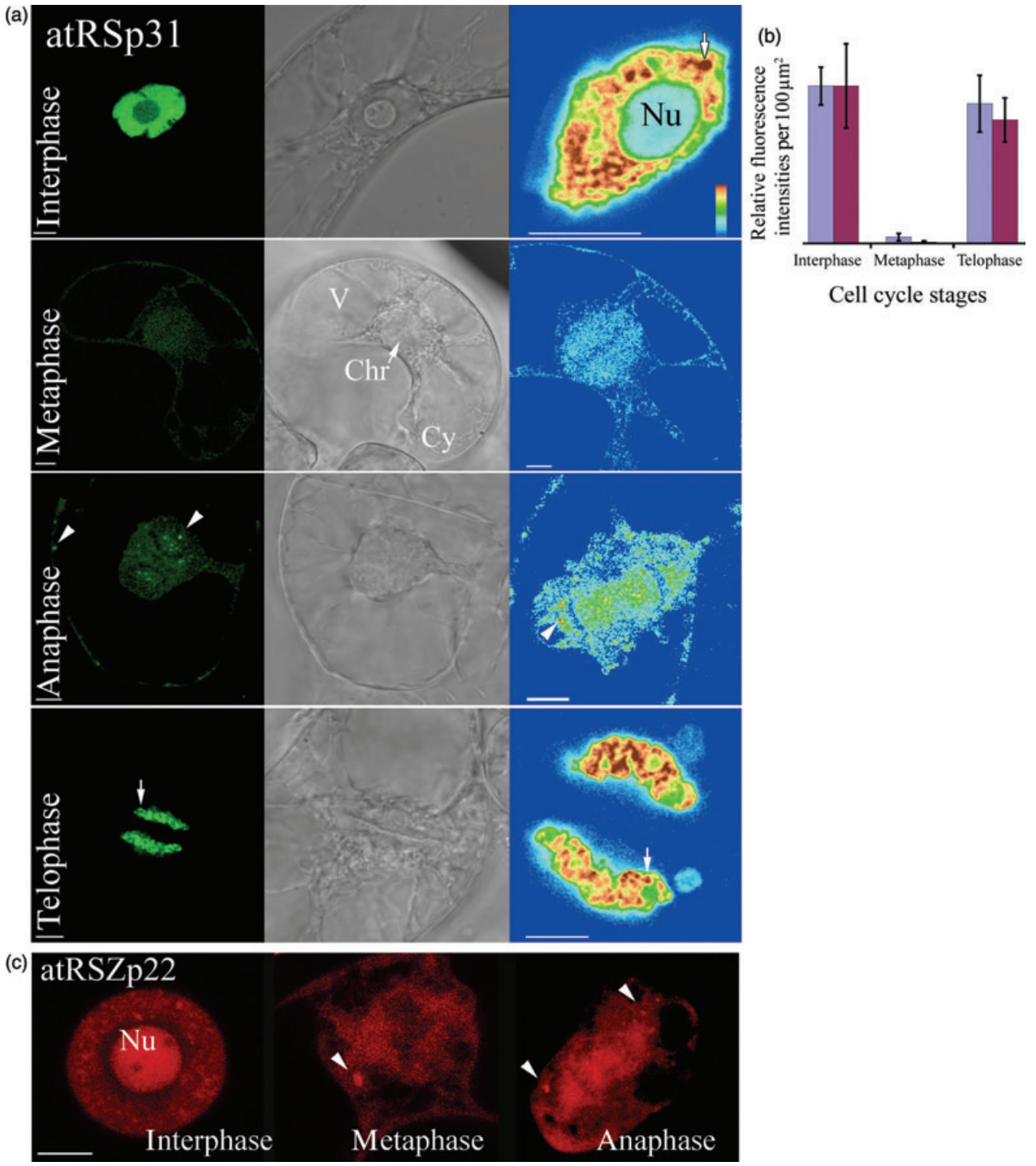

Figure 9. Cell cycle phase-dependent distribution of atRSp31-GFP (a, b) and atRSZp22-mRFP1 (c) in BY-2 cells.
(a) From left to right are confocal fluorescence images, transmission micrographs and pseudocolour fluorescence intensity obtained for enlarged central region of the cells. In interphase nuclei, atRSp31 displays a speckled pattern (arrow) while it is homogenously distributed at metaphase. At the anaphase stage, atRSp31-GFP concentrates in some tiny bright dots (arrowheads) in the area surrounding the chromosomes and in the cytoplasm. The speckles reappear at telophase (arrow).
(b) Graph showing the relative fluorescence intensities at different stages of the cell cycle (per 100 μm^2), interphase, metaphase and telophase. Two quantification methodologies are compared: in blue, quantification of average projections of entire nuclei and metaphase cells is performed, in purple, optical sections of *Z*-series are individually quantified (see Experimental procedures). The average values calculated for the interphase cells were set as 100% and the values obtained at the two other stages were expressed relative to this value. A tremendous decrease of atRSp31 is visible at metaphase; vertical bars are standard errors.
(c) AtRSZp22 shows nucleolar localization in some interphase nuclei and becomes enriched in one dot at metaphase and in more very tiny bright dots at anaphase (anaphase is a maximal projection of a *Z*-series). Nu, nucleolus; Chr, chromosomes; Cy, cytoplasm; V, vacuole. Scale bar, 8 μm.

Cell cycle

Little is known about the cell cycle phase-dependent distribution of SR proteins in plants. First, we analysed the localization of atRSp31 during mitosis in root tip meristems of young Arabidopsis transgenic seedlings. However, due to the small size of these cells, high resolution fluorescence distribution of atRSp31-GFP could not be acquired. Therefore, stably expressing tobacco BY-2 cells were generated. Due to their large nuclei and the possibility of synchronization, these cells are particularly convenient for such study. Confocal imaging has shown the detailed distribution of atRSp31-GFP at different stages of the cell cycle (Figure 9). AtRSp31-GFP displayed a speckled distribution in interphase nuclei of BY-2 cells. At metaphase, atRSp31-GFP was diffusely distributed throughout the cytoplasm and the intensity of the fusion protein decreased considerably. Quantification of fluorescence confirmed this observation with fluorescence intensity approximately 100 times weaker at metaphase than the one detected at interphase (Figure 9b). During anaphase, atRSp31-GFP became enriched in the cytoplasmic area largely surrounding the chromosomes and concentrated in tiny granules dispersed in the cytoplasm. At telophase, atRSp31-GFP localized exclusively in the nucleus in future daughter cells with a speckled distribution pattern, with no observation of labelling of the cytoplasm (Figure 9a). The fluorescence intensity at telophase was nearly identical to the one at interphase (Figure 9b). A similar distribution was observed in BY-2 cells expressing atRSZp22 with slight differences. A large number of interphase nuclei showed a nucleolar localization of atRSZp22 (Figure 9c). During metaphase, atRSZp22-mRFP1 localized in a diffuse pattern and sometimes concentrated in only one small structure resembling mammalian mitotic interchromatin granules (MIGs; see Discussion). More abundant and tiny foci were visible at anaphase.

Discussion

A plausible scenario for the colocalization of Arabidopsis SR proteins?

The SR proteins act at several steps in spliceosome assembly (Graveley, 2000). However, despite *in vitro* evidence, it is not yet clear how SR proteins interact with spliceosomal components in the native nuclear compartment, nor whether plant SR proteins are all targeted to the same nuclear speckle domains *in vivo*. The question is of interest in view of the fact that the capability for heterodimerization and heterotypic associations could provide potentially different SR factor complex formations with putative distinct pre-mRNA substrate specificity. Co-expression of Arabidopsis SR factors of different subclasses has been investigated *in vivo* by using *Agrobacterium*-mediated transient transformation. Despite slight differences in their nuclear distribution, our data suggest the overall subnuclear colocalization of SR factors in living plant cells within both the diffuse fraction and speckles, except for atRSZp22 (see later chapter). Could the most plausible scenario be an overall colocalization of SR proteins? The answer may be yes if we consider the preconceived concept that the RS domain of SR (and some SR-related) proteins is sufficient for targeting to speckles, that is speckles are non-specific storage/assembly sites of SR proteins. However, there is no direct evidence for such a role of speckles in plants and different RS domains can differentially target SR proteins to subnuclear domains (Neugebauer and Roth, 1997).

Our data suggest that ectopically expressed SR proteins are stably associated within nuclei irrespective of their molecular identity and rather independently of their phosphorylation state and of the transcriptional activity of the cell. The observation that ectopically expressed SR factors may associate in functional heterotypic complexes without any apparent specificity in their association raises the question of their functional redundancy. Regulating spliceosomal assembly and modulating levels of alternative splicing are undoubtedly important functions of SR proteins in metazoa. How is this done in plants? Cell-type-specific differences in Arabidopsis SR protein abundance – and consequently a distinct pattern of relative SR protein concentration – could be important for the regulation of (alternative) splicing of distinct pre-mRNAs. The transcriptional regulation of their temporal and spatial expression might also be of importance. Indeed, although overlapping expression patterns were observed in various cell types, the expression of most plant SR proteins was restricted to a particular cell/tissue (Kalyna *et al.*, 2003; Lopato *et al.*, 1999, 2002).

However, we are still considering the possibility of distinct heterotypic interactions of specific SR factors and their distinct RNA-binding specificities. In this regard, it is noteworthy that earlier reports showed that SR factors are detected at active sites of transcription, not necessarily coincident with speckles, and that specific SR proteins can be detected in only a subset of SR protein distribution (Neugebauer and Roth, 1997). Such differences in the localization of SR proteins might not be observed by using our approach because of overexpression of FP-tagged SR proteins. Moreover, RNA-binding specificities might be regulated by complex and cell-dependent post-translational modifications of SR proteins and associated factors. Therefore, it would be of interest to investigate possible cell type-dependent colocalization of SR proteins during plant development by using immunolocalization or gene-specific promoters and multiple fluorescence imaging.

Roles of Arabidopsis SR protein domains

Reports on the functional roles of the different domains of metazoan SR factors revealed striking differences in the localization and targeting signals present in SR proteins (Caceres *et al.*, 1997; Cazalla *et al.*, 2002; van Der Houven Van Oordt *et al.*, 2000; Hedley *et al.*, 1995). Nothing was known about the role of the plant SR protein domains in the control of their subcellular localization. Our findings provide evidence that the RS domains of Arabidopsis SR proteins are necessary for nuclear speckle targeting. In addition to this conserved feature between plant and animal SR proteins, we have identified potential functional differences as well. The deletion of the RS domain induces the instability of atRSp31 (but not of atRSZp22) which might be due to a folding problem of the fusion protein. This result suggests that the RS domain is possibly involved in the *in vivo* stability of atRSp31 through its level of phosphorylation (see later chapter on the cell cycle). Furthermore, we show that atRSZp22 lacking its RS domain was unexpectedly targeted into the nucleolus. An identical redistribution of wild type atRSZp22 was observed after inhibition of phosphorylation. Taken together, our findings strongly suggest that the RS domain of atRSZp22 regulates its shuttling between nucleoplasm and nucleolus through its level of phosphorylation. Such a transient nucleolar targeting could stress potential specific properties of this specific Arabidopsis SR protein (see next chapter).

Coexpression of wild type and mutant SR proteins shows that deletion of the RS domain of either atRSp31 or atRSZp22 does not alter the speckled distribution of other wild-type SR proteins. In contrast, RRM deleted atRSp31 is sufficient to target wild-type atRSZp22 to unusual nuclear subdomains. This result was surprising as the RRM domain is thought to determine substrate specificity. Moreover, we have observed that atRSp31 prevents the specific redistribution of atRSZp22 upon phosphorylation inhibition. Therefore, our results suggest that one specific SR protein (atRSp31) dragging along other SR factors in its distribution, might be dominant in the association and targeting events. It will be of interest to assess whether this 'dominant' character occurs with different combinations of mutant and wild-type SR factors in order to potentially determine the control of spliceosome assembly.

Arabidopsis SR protein: nucleolar or not nucleolar?

In eukaryotes, the nucleolus is the site of ribosome subunit biogenesis. The nucleolar proteome includes ribosomal RNA processing components and ribosomal proteins (Andersen *et al.*, 2002; Scherl *et al.*, 2002). Taken together, our data suggest that atRSZp22 associates, at least transiently, with nucleoli. As SR proteins would not be expected to concentrate in nucleoli, this finding raises several questions such as the functional significance or the importance of the nucleolar localization of this specific Arabidopsis SR factor.

It could be hypothesized that atRSZp22 contains a minimal sequence having homology with a nucleolar localization signal (perhaps the arginine and glycine-rich domain) and that its overexpression artefactually increases its nucleolar localization. In the endogenous wild-type atRSZp22, the putative nucleolar localization signal might be (partly) masked due to the RS domain. This hypothesis could explain the enrichment of RS domain-deleted atRSZp22 in the nucleolus.

However, one surprising finding of the past few years is the nucleolar localization of several molecules that are involved in non-nucleolar processes (Bernardi *et al.*, 2004; Lahmy *et al.*, 2004; Pederson, 1998; Politz *et al.*, 2000; Zhang *et al.*, 2004). Recent studies have indicated further additional functions for the nucleolus such as the assembly of the signal recognition particle RNP, the sequestration of regulatory molecules including cell cycle regulatory factors, or nuclear export processes in yeast (reviewed in Olson *et al.*, 2000; Pederson, 1998). Interestingly, a recent proteomic analysis of human nucleoli has identified many proteins involved in the regulation of (pre-)mRNA metabolism, including synthesis, editing, nuclear export and splicing processes (Scherl *et al.*, 2002). Among pre-mRNA splicing factors, the human heterogeneous nuclear ribonucleoprotein A1 and the SR protein SRp20 have been identified in the nucleolar proteome (Scherl *et al.*, 2002). Additional links between the nucleolus and pre-mRNA splicing have been suggested by the study of the dynamics of spliceosomal snRNAs/snRNPs and Cajal Bodies (Boudonck *et al.*, 1999; Gerbi and Lange, 2002; Trinkle-Mulcahy *et al.*, 2001). Conversely, the nucleolar protein NHPX has been shown to transiently accumulate in speckles prior to a later accumulation in nucleoli (Leung and Lamond, 2002).

It is tempting to suggest an mRNA export function to atRSZp22 assuming that the nucleolus in higher eukaryotes is involved in this process and that atRSZp22 binds to poly(A)+ RNA as a component of the exon-exon junction complex, for example. In yeast, the function of the nucleolus in mRNA export is well documented (Ideue *et al.*, 2004). In higher eukaryotes, a major involvement of the nucleolus for this process has not been reported although earlier studies have shown that inactivation of HeLa nucleoli inhibits the export of non-ribosomal RNA (Deak, 1973). Interestingly, the proteomic analysis of the human nucleolus has identified mRNA nucleo-cytoplasmic export proteins, such as Polypyrimidine tract binding protein (PTB/hnRNP I), a member of the hnRNP family, or Aly/REF, a cellular export factor which remains bound to the spliced transcripts to direct them to the TAP/nuclear export factor 1 (NXF1) nuclear export pathway (Andersen *et al.*, 2002; Kim *et al.*, 2001; Scherl *et al.*, 2002). Moreover, the hypophosphorylated SR protein 9G8 has higher affinity for the export receptor TAP/NXF1 (Huang

et al., 2004). In yeast, Npl3p (Nop3p) is an SR-like protein required for mRNA export and is localized both in the nucleoplasm and nucleolus (Gilbert and Guthrie, 2004; Lee *et al.*, 1996; Russell and Tollervey, 1995). Besides their role in pre-mRNA splicing (and mRNA export) plant SR proteins might have other functions yet to be defined. For instance, the human SRp38 recorded as an SR splicing factor functions more as a general repressor of splicing when dephosphorylated (Shin *et al.*, 2004). Possible functional interrelations between nucleoli and splicing speckles in plants would need nevertheless to be further experimentally defined.

Dynamics of SR factors in interphase nuclei and during the plant cell cycle

We demonstrate that *Agrobacterium*-mediated transient transformation can be used to investigate the (co)localization of SR splicing factors and of other nuclear regulatory proteins in both tobacco and Arabidopsis cells. The FP-based assay also provides a powerful tool for the study of the dynamics of SR factors by using FRAP which emphasizes the high dynamic properties of plant SR proteins in interphase nucleus.

In mammals, SR proteins become diffusely distributed at metaphase and concentrated in MIGs (Lamond and Spector, 2003). Although their functions remain unclear, MIGs have been suggested to be the counterparts of interphase speckles (Lamond and Spector, 2003). Herein, we investigate the reorganization of SR splicing factors during the cell cycle in tobacco BY-2 cells. In contrast to previously reported observations describing an homogenous distribution of atSRp34 (Fang *et al.*, 2004), we show that atRSZp22 and atRSp31, in addition to a homogeneous distribution, concentrated in small bright fluorescent granules mainly at the anaphase stage. Whether these mitotic bright dots have similar functions as (and correspond to) mammalian MIGs remain to be shown.

The fluorescence of atRSp31-GFP strongly decreases at metaphase suggesting that atRSp31 could be the subject of proteolysis during the cell cycle. Interestingly, human SRp55 has been shown to be specifically targeted for degradation under Clk/Sty kinase overexpression, most likely via the ubiquitin-mediated proteolytic pathway (Lai *et al.*, 2003). The degradation of SRp55 appears to be regulated by the RS domain probably via phosphorylation. The phosphorylation of the RS domain regulates the spatial distribution of SR proteins during the cell cycle as well (Gui *et al.*, 1994; Lamond and Spector, 2003).

In summary, this study demonstrates functionally conserved features of SR splicing regulators among metazoa and plants, and different properties of Arabidopsis SR proteins. Future study of the dynamic distribution of SR factors should continue to provide valuable insight into their functional organization, and subsequently a better understanding of the compartmentalization of the plant cell nucleus.

Experimental procedures

Materials

Arabidopsis thaliana and *Nicotiana tabacum* (cv. Petit Havana) seeds were sown on soil in a culture chamber and allowed to germinate and grow under long-day conditions (16-h-light/8-h-dark photoperiod) at approximately 20°C. Arabidopsis plants with well-developed leaf rosette and 20-cm-high tobacco plants were used for *Agrobacterium*-mediated transient expression. Tobacco (*N. tabacum*) BY-2 cells were grown at 28°C by weekly dilution in fresh BY-2 medium, consisting of 0.44% (w/v) of Murashige and Skoog (MS) salts supplemented with 3% (w/v) sucrose, 0.2 mg ml^{-1} KH_2PO_4, 50 μg ml^{-1} myo-inositol, 2.5 μg ml^{-1} thiamine-HCl, 0.2 μg ml^{-1} 2,4-dichlorophenoxy acetic acid (2,4-D), adjusted to pH 5.8 with 1 M KOH. BY-2 cells were maintained in the dark with continuous shaking.

RNA extraction and RT-PCR

Extraction of total RNA was carried out by the hot phenol method and LiCl precipitation as described previously (Shirzadegan *et al.*, 1991). The RNA pellet was dissolved in 10 mM Tris–HCl, pH 7.5 and 1 mM EDTA after ethanol precipitation. Poly(A)+ mRNA was purified with the Oligotex mRNA kit (Qiagen, Venlo, The Netherlands). RT-PCR amplification was performed on either 0.5–1 μg of total RNA or 0.25–0.5 μg of poly (A)+ mRNA by using PowerScript (Clontech, Palo Alto, CA, USA) with oligo-d(T) primer. The resulting cDNAs were used as templates for PCR amplification with gene-specific primers or modified primers for subsequent cloning in binary vectors.

Binary vector construction and sequence analysis

The construction of pBAR35S::atRSp31-GFP was described in a previous report (Docquier *et al.*, 2004). For all constructs, coding sequences were amplified from the appropriate source by PCR using the proofreading Pfu polymerase (Promega, Leiden, The Netherlands). *AtRSp31::GFP* fusions with different deletions in the *atRSp31* coding sequence were constructed as follows. The coding sequences of the chimeric mutants ΔRNP2-GFP and ΔRRM-GFP were amplified directly from pBAR35S::atRSp31-GFP (with respectively the 5′ primers 5′-ATGTCTGGATATGCTTTTGTGTACTTT-3′ and 5′-ATGTGGGCAAAGGGTGAACGT-3′, and the 3′ primer 5′-TTACTTGTACAGCTCGTCCATGC-3′), and cloned into the blunt-ended *Sma*I binary vector pBAR35S, carrying the cauliflower mosaic virus 35S (CaMV35S) promoter/terminator (Docquier *et al.*, 2004). The coding sequences of ΔRS and ΔIR/RS were amplified from pBAR35S::atRSp31-GFP (using the 5′ primer 5′-ATGAGGCCAGTGTTCGTCGGC-3′, and respectively, the 3′ primers 5′-GAAGATCTTCCGGAGGAAACAACCCTATC-3′ and 5′-GAAGATCTTCCGGATTCAACTGATAACTTGCGTTTCTC-3′, both containing a *Bgl*II site, underlined). The coding sequence of *EGFP* was amplified from pEGFP (Clontech) with the 5′ primer 5′-GAAGATCTATGGTGAGCAAGGGCGAGGAG-3′ containing a *Bgl*II site, and the 3′ primer 5′-TTACTTGTACAGCTCGTCCATGC-3′. The resulting PCR fragments were digested with *Bgl*II and ligated. The chimeric gene was then amplified and cloned into pBAR35S. As selection of BY-2 cell transformants could not be performed based on glufosinate ammonium resistance (conferred by the *Bar* gene in pBAR35S plasmid), the pBI121 (Clontech) vector was subsequently used for further transformations. Plasmid pBI121, carrying a CaMV 35S–β-glucuronidase–nopaline synthase

(35S-GUS-NOS) expression cassette with a kanamycin resistance gene as a selectable marker for plant cell transformation, was first digested with *Bam*HI and *Sst*I to remove the GUS coding sequence generating pBI35S-ΔGUS. AtRSp31-GFP (amplified from pBAR35S::atRSp31-GFP using upward and forward primers containing BamHI and SstI sites respectively) was cloned into pBI-ΔGUS yielding pBI35S::atRSp31-GFP.

To study the colocalization of SR factors, multiple fluorescence imaging was performed by using m(onomeric)RFP1 (a derivative of DsRed; a kind gift from Prof. R. Tsien, Howard Hughes Medical Institute Laboratories, University of California; Campbell *et al.*, 2002). For the construction of pBI35S::atRSZp22-mRFP1, mRFP1 was amplified using the 5′ primer (5′-GTGGTACCATGG-CCTCCTCCGAGGACGTCATC-3′) containing a *Kpn*I site, and the 3′ primer (5′-TCGAGCTCTTAGGCGCCGGTGGAGTGGCG-3′) containing an *Sst*I site, and for pBI35S::atRSZp22-GFP the EGFP coding sequence was amplified from pEGFP (using the 5′ primer 5′-GTGGTACCATGGTGAGCAAGGGCGAGGAG-3′, containing a *Kpn*I site and the 3′ primer 5′-TCGAGCTCTTACTTGTACAGCTCGTCC-ATGCCGAGAGTGAT-3′ containing an *Sst*I site). AtRSZp22 was amplified by RT-PCR using the 5′ primer (5′-CGGGATCCAA-GGAGATATAACAATGTCACGTGTGTACCTCGG-3′) containing a *Bam*HI site and the 3′ primer (5′-GTGGTACCACCACCGCT-CCTGCTTCTGCGTCT-3′) containing a *Kpn*I site. The amplified fragments were then digested with *Kpn*I and ligated. The chimeric gene was then PCR amplified and cloned into pBI-ΔGUS. We followed the same approach for the construction of pBI35S:: atRSZ33-GFP and pBI35S::atRSZ33-mRFP1 by using the atRSZ33-specific primers (5′-CGGGATCCAACAATGCCTCGCTATGATGAT-CGCTA-3′, containing a *Bam*HI site and 5′-GTGGTACCACCA-CCAGGAGACTCACTTCCTCTAGGGGAAG-3′, containing a *Kpn*I site), and of pBI35S::atSRp34-GFP by using the atSRp34-specific primers (5′-CGGGATCCAAGGAGATATAACAATGAGCAGTCGTTC-GAGTA-3′, containing a *Bam*HI site and 5′-GGGGTACCCCTCGATG-GACTCCTAGTG-3′, containing a *Kpn*I site). The *Arabidopsis Rpb15.9* sequence was amplified by RT-PCR (using primers 5′-GTGGTACCATGTCCGGAGAAGAAGAA-3′ containing a *Kpn*I site, and 5′-CTACTCGAATCTCTTGACAAGTGAGAG-3′). The *GFP* sequence was amplified with 5′-GCTCTAGAATGGTGAGCAAGGGC-GAG-3′, containing an *Xba*I site and 5′-GTGGTACCACCA-CCCTTGTACAGCTCGTCCAT-3′ containing a *Kpn*I site. The resulting PCR products were digested with *Kpn*I and ligated. The chimeric sequence was then amplified, digested with *Xba*I and cloned into pBI-ΔGUS (which was first refilled with Klenow after *Sst*I digestion). In the resulting vector designated pBI*35S::GFP-Rpb15.9*, Rpb15.9 is fused to the C-terminal end of GFP.

The resultant plasmids were electroporated into the *Agrobacterium tumefaciens* strain GV3101 (pMP90), and subsequently used for transformations. Independent clones were sequenced to detect any mutation caused by PCR. The SMART prediction program (Letunic *et al.*, 2004; http://smart.embl-heidelberg.de/) was used for domain prediction and their precise location.

Agrobacterium tumefaciens-mediated transient expression

Transient transformation in tobacco and Arabidopsis leaves was performed essentially as described previously (Docquier *et al.*, 2004). Briefly, *A. tumefaciens* bearing the appropriate binary vector was grown at 28°C overnight in 10 ml YEB liquid medium (0.5% sucrose, 0.1% yeast extract, 0.5% Bactopeptone, 0.5% Invitrogen beef extract, 2 mM $MgSO_4$, pH 7.4) supplemented with 25 μg ml^{-1} gentamycin, 100 μg ml^{-1} rifampicin and 50 μg ml^{-1} kanamycin. After centrifugation, the bacteria were washed with infiltration medium (50 mM Mes, 2 mM Na_3PO_4, 0.5% glucose and 100 μM acetosyringone) and then resuspended in the same medium at the desired final OD_{600}. Leaves were infiltrated using a 5-ml syringe by applying gentle pressure through the stomata of the abaxial epidermis. For coexpression, various co-inoculation experiments and *Agrobacterium* densities were tested on tobacco. The most efficient cell cotransformation was obtained with inocula of OD_{600} ranging between 0.6 and 1.0; high inoculum densities (OD_{600} above 1.3) prevented transformation. Inoculated plants were then incubated under normal growth conditions. The infiltrated areas were cut at 48–72 h after inoculation and further processed for imaging or inhibitor treatments.

Arabidopsis and BY-2 cell transformation

Arabidopsis plant transformation was performed as described previously (Docquier *et al.*, 2004). Transgenic T_1 plants were selected on plates containing sterile solidified MS medium supplemented with 3% sucrose and 50 μg ml^{-1} glufosinate ammonium (Riedel-de-Haën, Sigma-Aldrich, Bornem, Belgium). After 10 days of growth, transformants were planted directly into soil at the two-leaf stage to obtain T_2 and T_3 progeny.

Stable transformation and synchronization of BY-2 cells was performed essentially as described previously (Grec *et al.*, 2003). Briefly, 4 ml of a 3-day-old cell culture were distributed into a Petri dish and 0.1 ml of an overnight *Agrobacterium* culture, containing the binary vector of interest, was added. After 4 days of coincubation at 22°C, BY-2 cells were washed three times with 10 ml of BY-2 medium and plated onto sterile solidified BY-2 medium supplemented with 100 μg ml^{-1} kanamycin, and 500 μg ml^{-1} carbenecillin. Plates were incubated for 3–4 weeks at 28°C until transformed calli were visible. Transgenic calli were screened for their expression using confocal microscopy and selected cell colonies were further transferred onto new selective plates.

Inhibitor treatment

Fragments of transiently transformed leaves were used for inhibitor treatments as described previously (Docquier *et al.*, 2004). Leaf tissues were floated in 10 μM α–amanitin (Sigma), 500 nM okadaic acid (Calbiochem, La Jolla, CA, USA), 50 μM staurosporine (Sigma) or water as control for various time periods.

Antibodies and indirect immunofluorescence

The subcellular localization of phosphorylated RNAP II C-terminal domain (CTD) was determined using H5 mouse monoclonal antibodies (Covance Research Products, Berkeley, CA, USA). The H5 antibodies mark the RNAP II phosphorylated at serine 2 of the CTD of the largest RNAP II subunit. For immunofluorescence analysis, fragments of Arabidopsis and tobacco leaf cells were fixed overnight in 4% paraformaldehyde in 1x PEM buffer (50 mM PIPES, NaOH, pH 7.0; 5 mM EGTA; 5 mM $MgSO_4$), and washed two times with PEM supplemented with 0.1% Triton X-100. The cells were incubated in driselase (0.25%), cellulase (1%) and pectinase (1%) for 2 h at room temperature. After washing in Triton X-100 PEM, cells were then incubated for 1 h with a blocking solution consisting of 1% BSA, 5% normal goat serum in PBS at room temperature. Fixed cells were incubated overnight with H5 antibodies at a dilution of 1:100. After washing, primary antibodies were detected using FITC- or Alexa 633-conjugated goat anti-mouse antibody at dilution of 1:100 and 1:500, respectively, with an incubation time of at least 1 h. Nuclei were counterstained with DAPI.

Fluorescence microscopy

For epifluorescence microscopy, images were captured with a Nikon CoolPix 950 digital camera (Nikon, Tokyo, Japan). For confocal imaging, images were acquired using a Leica TCS SP2 inverted confocal laser microscope (Leica Microsystems, Heidelberg, Germany) equipped with one argon and two helium–neon lasers. Digitized images were acquired using a 63 × NA1.5 Plan-Apo water-immersion objective at 1024 × 1024 pixel resolution. The diameter of the pinhole was set up equal to the Airy unit. Series of optical sections were carried out to analyse the spatial distribution of fluorescence, and for each nucleus, they were recorded with a *Z*-step ranging between 0.2 and 0.5 μm. Images were acquired under identical conditions and we ensured that the maximal fluorescence signal was not saturating the photomultiplier tubes (PMT). For multicolour imaging, GFP was visualized by using an excitation wavelength of 488 nm and the emission light was dispersed and recorded at 500–535 nm. MonomericRFP1 was detected by using an excitation wavelength of 543 and the 488/543 dichroic mirror, and the mRFP1 emission was dispersed and recorded at 585–660 nm. The acquisition was set up to avoid any crosstalk of the two fluorescence emissions. To quantify the fluorescence, lines were drawn through the nucleus by using Leica software (version 2.5). The fluorescence intensities along this line, represented by a graph profile, provide data on the relative concentration of FP-tagged SR factors in the subnuclear compartments.

After a period of observation of over 2 h, abnormal localization of SR proteins was observed possibly due to experimental stress such as hypoxia followed by ATP depletion, and/or cold temperature. Our system does not bear a temperature-control unit or objective heaters, and as well known, the objective and the optical coupling medium act as a thermal conductive object/medium sinking heat away from the specimen.

To perform FRAP experiments, transgenics Arabidopsis seedlings (T_2 and T_3) and tobacco leaf fragments stably and transiently expressing atRSp31-GFP, respectively, were mounted in water and observed using the 488-nm line of the argon laser in conjunction with a Plan-Apo 100× 1.4 NA oil immersion objective. Nuclei ($n = 5$ per experiment) were imaged at medium resolution of 512 × 512 pixels. Using the extended time-lapse function, pre-bleach images (generally, between five and 10 data points) were acquired by sequentially scanning the same optical section through the nucleus at low laser power (3–5% transmission). Next, the laser was zoomed in square areas (from 10 to 20 μm^2) with power increased to 100% and the area was scanned four to six times until the fluorescence was significantly reduced. The laser was zoomed out and its power reduced to pre-bleach settings. Recovery of fluorescence intensity was monitored by scanning the nucleus until the recovery reached a steady plateau. Nuclear areas ranging from 10 to 20 μm^2, corresponding approximately to 8–15% of the surface of the nucleus, were bleached and recovery rates did not appear to be dependent on the size of the bleached region. We ensure that post-bleach imaging did not result in significant loss of fluorescence over time. The values of the bleached areas were then normalized and further analysed by using GraphPad Prism 4 and non-linear sigmoidal regression (GraphPad Software, San Diego, CA, USA).

For quantification of fluorescence in BY-2 cells, the maximum fluorescence intensity was first determined by scanning different stages of the cell cycle (interphase, metaphase and telophase), and we ensured that this maximal fluorescence signal was not saturating the PMT. *Z*-series (with a *Z*-step of 1 μm) of nuclei and metaphase cells ($n = 6$) were then collected keeping constant all parameters (laser intensity, PMT gain, scanning speed, etc.). The fluorescence intensities of individual optical sections were quantified by delineating the nucleus (interphase and telophase) or the cytoplasm (metaphase) using Leica software. On the basis of the collected image stacks, fluorescence intensities were averaged to produce a mean fluorescence intensity for each cell and the pixel value per unit area (100 μm^2) was calculated. These values were averaged within groups for the various mitotic stages and standard errors were calculated in Microsoft Excel. The average value calculated for the interphase cells was set as 100% and the other values were expressed relative to this. For comparison, quantification was also performed on an average projection for each of the series collected. The average pixel intensity of confocal reconstructions of either the entire nucleus (interphase and telophase) or the entire metaphase cell was measured using Leica software and the pixel values per 100 μm^2 were averaged for each stage of the cell cycle.

Captured images were exported as TIFF format files and further processed using Adobe Photoshop 7.0 for figure mounting and labelling purposes.

Acknowledgements

We are grateful to Prof. Roger Y. Tsien (Howard Hughes Medical Institute Laboratories, University of California, San Diego) for providing the plasmid containing mRFP1, and to Prof. Marc Boutry (Université Catholique de Louvain, Belgium) for providing the tobacco BY-2 cells and for valuable advice on transformation. This research was supported by grants from 'National Fund for Scientific Research' (grants No. 2.4520.02 and 2.4542.00) and from 'Fonds Spéciaux du Conseil de la Recherche' of the University of Liège to PM. VT is supported by Fonds de la Recherche pour l'Industrie et l'Agriculture (FRIA).

Supplementary Material

The following material is available from http://www.blackwellpublishing.com/products/journals/suppmat/TPJ/TPJ2321/TPJ2321sm.htm

Figure S1. Localization of Arabidopsis FP-tagged SR proteins in nuclei of transiently expressing cells under experimental stress. AtRSp31 is aggregated into numerous speckles in the nucleoplasm which concentrate around the nucleolus; atRSZp22 is strongly accumulated in the nucleolus with a more homogenous distribution in nucleoplasmic pool. Nu, nucleolus. Scale bar, 4 μm.

Figure S2. Comparison of the nuclear distribution of individually expressed FP-tagged atRSp31 and atRSZ33 with their localization in co-expressing cells. (a) When expressed alone, atRSp31 distributes more in dot-like speckles (arrows) while atRSZ33 forms long intranuclear tracks (arrowheads) interconnecting irregularly shaped speckles. In coexpressing cells, atRSp31 and atRSZ33 colocalize in nuclear domains of intermediate shape between dot-like speckles and intranuclear tracks; this observation emphasizes their association in nuclei. Nu, nucleolus. Scale bars, 4 μm.

Figure S3. Comparison of the redistribution of FP-tagged atRSZp22 and atRSp31 in tobacco nuclei. After staurosporine treatment, atRSZp22 accumulates in the nucleolus (right) while atRSp31 concentrates in numerous speckles and around the nucleolus (left). Nu, nucleolus. Scale bar, 4 μm.

References

Ali, G.S., Golovkin, M. and Reddy, A.S. (2003) Nuclear localization and in vivo dynamics of a plant-specific serine/arginine-rich protein. *Plant J.* **36**, 883–893.

Andersen, J.S., Lyon, C.E., Fox, A.H., Leung, A.K., Lam, Y.W., Steen, H., Mann, M. and Lamond, A.I. (2002) Directed proteomic analysis of the human nucleolus. *Curr. Biol.* **12**, 1–11.

Bernardi, R., Scaglioni, P.P., Bergmann, S., Horn, H.F., Vousden, K.H. and Pandolfi, P.P. (2004) PML regulates p53 stability by sequestering Mdm2 to the nucleolus. *Nat. Cell Biol.* **6**, 665–672.

Boudonck, K., Dolan, L. and Shaw, P.J. (1998) Coiled body numbers in the Arabidopsis root epidermis are regulated by cell type, developmental stage and cell cycle parameters. *J. Cell Sci.* **111**, 3687–3694.

Boudonck, K., Dolan, L. and Shaw, P.J. (1999) The movement of coiled bodies visualized in living plant cells by the green fluorescent protein. *Mol. Biol. Cell*, **10**, 2297–2307.

Brown, J.W.S. and Simpson, C.G. (1998) SPLICE SITE SELECTION IN PLANT PRE-mRNA SPLICING. *Annu. Rev. Plant Physiol. Plant Mol. Biol.* **49**, 77–95.

Caceres, J.F., Misteli, T., Screaton, G.R., Spector, D.L. and Krainer, A.R. (1997) Role of the modular domains of SR proteins in subnuclear localization and alternative splicing specificity. *J. Cell Biol.* **138**, 225–238.

Campbell, R.E., Tour, O., Palmer, A.E., Steinbach, P.A., Baird, G.S., Zacharias, D.A. and Tsien, R.Y. (2002) A monomeric red fluorescent protein. *Proc. Natl Acad. Sci. USA*, **99**, 7877–7882.

Cazalla, D., Zhu, J., Manche, L., Huber, E., Krainer, A.R. and Caceres, J.F. (2002) Nuclear export and retention signals in the RS domain of SR proteins. *Mol. Cell Biol.* **22**, 6871–6882.

Deak, I.I. (1973) Further experiments on the role of the nucleolus in the transfer of RNA from nucleus to cytoplasm. *J. Cell Sci.* **13**, 395–401.

van Der Houven Van Oordt, W., Newton, K., Screaton, G.R. and Caceres, J.F. (2000) Role of SR protein modular domains in alternative splicing specificity in vivo. *Nucleic Acids Res.* **28**, 4822–4831.

Docquier, S., Tillemans, V., Deltour, R. and Motte, P. (2004) Nuclear bodies and compartmentalization of pre-mRNA splicing factors in higher plants. *Chromosoma*, **112**, 255–266.

Fang, Y., Hearn, S. and Spector, D.L. (2004) Tissue-specific expression and dynamic organization of SR splicing factors in Arabidopsis. *Mol. Biol. Cell*, **15**, 2664–2673.

Gama-Carvalho, M., Krauss, R.D., Chiang, L., Valcarcel, J., Green, M.R. and Carmo-Fonseca, M. (1997) Targeting of U2AF65 to sites of active splicing in the nucleus. *J. Cell Biol.* **137**, 975–987.

Gama-Carvalho, M., Carvalho, M.P., Kehlenbach, A., Valcarcel, J. and Carmo-Fonseca, M. (2001) Nucleocytoplasmic shuttling of heterodimeric splicing factor U2AF. *J. Biol. Chem.*, **276**, 13104–13112.

Gerbi, S.A. and Lange, T.S. (2002) All small nuclear RNAs (snRNAs) of the [U4/U6.U5] Tri-snRNP localize to nucleoli; Identification of the nucleolar localization element of U6 snRNA. *Mol. Biol. Cell*, **13**, 3123–3137.

Gilbert, W. and Guthrie, C. (2004) The Glc7p nuclear phosphatase promotes mRNA export by facilitating association of Mex67p with mRNA. *Mol. Cell*, **13**, 201–212.

Graveley, B.R. (2000) Sorting out the complexity of SR protein functions. *RNA*, **6**, 1197–1211.

Grec, S., Vanham, D., de Ribaucourt, J.C., Purnelle, B. and Boutry, M. (2003) Identification of regulatory sequence elements within the transcription promoter region of NpABC1, a gene encoding a plant ABC transporter induced by diterpenes. *Plant J.* **35**, 237–250.

Gui, J.F., Lane, W.S. and Fu, X.D. (1994) A serine kinase regulates intracellular localization of splicing factors in the cell cycle. *Nature*, **369**, 678–682.

Hedley, M.L., Amrein, H. and Maniatis, T. (1995) An amino acid sequence motif sufficient for subnuclear localization of an arginine/serine-rich splicing factor. *Proc. Natl Acad. Sci. USA*, **92**, 11524–11528.

Huang, Y., Yario, T.A. and Steitz, J.A. (2004) A molecular link between SR protein dephosphorylation and mRNA export. *Proc. Natl Acad. Sci. USA*, **101**, 9666–9670.

Ideue, T., Azad, A.K., Yoshida, J., Matsusaka, T., Yanagida, M., Ohshima, Y. and Tani, T. (2004) The nucleolus is involved in mRNA export from the nucleus in fission yeast. *J. Cell Sci.* **117**, 2887–2895.

Kalyna, M. and Barta, A. (2004) A plethora of plant serine/arginine-rich proteins: redundancy or evolution of novel gene functions? *Biochem. Soc. Trans.* **32**, 561–564.

Kalyna, M., Lopato, S. and Barta, A. (2003) Ectopic expression of atRSZ33 reveals its function in splicing and causes pleiotropic changes in development. *Mol. Biol. Cell*, **14**, 3565–3577.

Kim, V.N., Yong, J., Kataoka, N., Abel, L., Diem, M.D. and Dreyfuss, G. (2001) The Y14 protein communicates to the cytoplasm the position of exon-exon junctions. *Embo J.* **20**, 2062–2068.

Kimura, M., Sakurai, H. and Ishihama, A. (2001) Intracellular contents and assembly states of all 12 subunits of the RNA polymerase II in the fission yeast *Schizosaccharomyces pombe*. *Eur. J. Biochem.* **268**, 612–619.

Kramer, A. (1996) The structure and function of proteins involved in mammalian pre-mRNA splicing. *Annu. Rev. Biochem.* **65**, 367–409.

Lahmy, S., Guilleminot, J., Cheng, C.M., Bechtold, N., Albert, S., Pelletier, G., Delseny, M. and Devic, M. (2004) DOMINO1, a member of a small plant-specific gene family, encodes a protein essential for nuclear and nucleolar functions. *Plant J.* **39**, 809–820.

Lai, M.C., Lin, R.I. and Tarn, W.Y. (2003) Differential effects of hyperphosphorylation on splicing factor SRp55. *Biochem J.* **371**, 937–945.

Lamond, A.I. and Spector, D.L. (2003) Nuclear speckles: a model for nuclear organelles. *Nat. Rev. Mol. Cell Biol.* **4**, 605–612.

Larkin, R.M. and Guilfoyle, T.J. (1998) Two small subunits in Arabidopsis RNA polymerase II are related to yeast RPB4 and RPB7 and interact with one another. *J. Biol. Chem.* **273**, 5631–5637.

Lee, M.S., Henry, M. and Silver, P.A. (1996) A protein that shuttles between the nucleus and the cytoplasm is an important mediator of RNA export. *Genes Dev.* **10**, 1233–1246.

Letunic, I., Copley, R.R., Schmidt, S., Ciccarelli, F.D., Doerks, T., Schultz, J., Ponting, C.P. and Bork, P. (2004) SMART 4.0: towards genomic data integration. *Nucleic Acids Res.* **32** (Database issue), D142–D144.

Leung, A.K. and Lamond, A.I. (2002) In vivo analysis of NHPX reveals a novel nucleolar localization pathway involving a transient accumulation in splicing speckles. *J. Cell Biol.* **157**, 615–629.

Lopato, S., Waigmann, E. and Barta, A. (1996) Characterization of a novel arginine/serine-rich splicing factor in Arabidopsis. *Plant Cell*, **8**, 2255–2264.

Lopato, S., Kalyna, M., Dorner, S., Kobayashi, R., Krainer, A.R. and Barta, A. (1999) atSRp30, one of two SF2/ASF-like proteins from *Arabidopsis thaliana*, regulates splicing of specific plant genes. *Genes Dev.* **13**, 987–1001.

Lopato, S., Forstner, C., Kalyna, M., Hilscher, J., Langhammer, U., Indrapichate, K., Lorkovic, Z.J. and Barta, A. (2002) Network of interactions of a novel plant-specific Arg/Ser-rich protein, atRSZ33, with atSC35-like splicing factors. *J. Biol. Chem.* **277**, 39989–39998.

Melcak, I., Cermanova, S., Jirsova, K., Koberna, K., Malinsky, J. and Raska, I. (2000) Nuclear pre-mRNA compartmentalization: trafficking of released transcripts to splicing factor reservoirs. *Mol. Biol. Cell*, **11**, 497–510.

Misteli, T. (2000) Cell biology of transcription and pre-mRNA splicing: nuclear architecture meets nuclear function. *J. Cell Sci.* **113**, 1841–1849.

Neugebauer, K.M. and Roth, M.B. (1997) Distribution of pre-mRNA splicing factors at sites of RNA polymerase II transcription. *Genes Dev.* **11**, 1148–1159.

Olson, M.O., Dundr, M. and Szebeni, A. (2000) The nucleolus: an old factory with unexpected capabilities. *Trends Cell Biol.* **10**, 189–196.

Pederson, T. (1998) The plurifunctional nucleolus. *Nucleic Acids Res.* **26**, 3871–3876.

Phair, R.D. and Misteli, T. (2000) High mobility of proteins in the mammalian cell nucleus. *Nature*, **404**, 604–609.

Politz, J.C., Yarovoi, S., Kilroy, S.M., Gowda, K., Zwieb, C. and Pederson, T. (2000) Signal recognition particle components in the nucleolus. *Proc. Natl Acad. Sci. USA*, **97**, 55–60.

Prasanth, K.V., Sacco-Bubulya, P.A., Prasanth, S.G. and Spector, D.L. (2003) Sequential entry of components of the gene expression machinery into daughter nuclei. *Mol. Biol. Cell*, **14**, 1043–1057.

Reddy, A.S.N. (2001) Nuclear pre-mRNA splicing in plants. *Crit. Rev. Plant Sci.* **20**, 523–571.

Russell, I. and Tollervey, D. (1995) Yeast Nop3p has structural and functional similarities to mammalian pre-mRNA binding proteins. *Eur. J. Cell Biol.* **66**, 293–301.

Sacco-Bubulya, P. and Spector, D.L. (2002) Disassembly of interchromatin granule clusters alters the coordination of transcription and pre-mRNA splicing. *J. Cell Biol.* **156**, 425–436.

Savaldi-Goldstein, S., Sessa, G. and Fluhr, R. (2000) The ethylene-inducible PK12 kinase mediates the phosphorylation of SR splicing factors. *Plant J.* **21**, 91–96.

Scherl, A., Coute, Y., Deon, C., Calle, A., Kindbeiter, K., Sanchez, J.C., Greco, A., Hochstrasser, D. and Diaz, J.J. (2002) Functional proteomic analysis of human nucleolus. *Mol. Biol. Cell*, **13**, 4100–4109.

Shin, C., Feng, Y. and Manley, J.L. (2004) Dephosphorylated SRp38 acts as a splicing repressor in response to heat shock. *Nature*, **427**, 553–558.

Shirzadegan, M., Christie, P. and Seemann, J.R. (1991) An efficient method for isolation of RNA from tissue cultured plant cells. *Nucleic Acids Res.* **19**, 6055.

Trinkle-Mulcahy, L., Sleeman, J.E. and Lamond, A.I. (2001) Dynamic targeting of protein phosphatase 1 within the nuclei of living mammalian cells. *J. Cell Sci.* **114**, 4219–4228.

Yeakley, J.M., Tronchere, H., Olesen, J., Dyck, J.A., Wang, H.Y. and Fu, X.D. (1999) Phosphorylation regulates in vivo interaction and molecular targeting of serine/arginine-rich pre-mRNA splicing factors. *J. Cell Biol.* **145**, 447–455.

Zhang, S., Hemmerich, P. and Grosse, F. (2004) Nucleolar localization of the human telomeric repeat binding factor 2 (TRF2). *J. Cell Sci.* **117**, 3935–3945.